A Wideband, Low Profile, Shorted Top Hat Monocone Antenna

Daniel W. Aten, *Member, IEEE*, and Randy L. Haupt, *Fellow, IEEE*

***Abstract*—A new, innovative, wideband antenna design which is short compared to wavelength and has an omni-directional radiation pattern that is theta polarized is investigated. The antenna design is a shorted top hat monocone that is $\lambda/14.7$ tall and has a 3:1 bandwidth. The bandwidth of the antenna was optimized by a genetic algorithm. To verify the results, a prototype was built. Modeled and measured results compared well. A link budget analysis was also performed to verify that the design performed as well or better than a monopole.**

***Index Terms*—Antenna measurements, broadband antennas, communication system performance, communication systems, electrically small antennas, monopole antennas.**

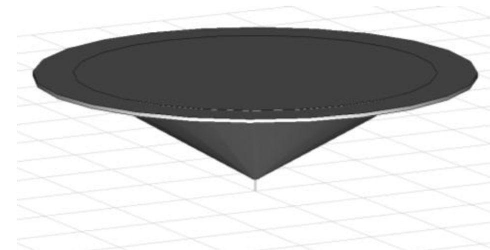

Fig. 1. An optimized design on an infinite ground plane without shorting pins.

I. Introduction

Many communication and sensing systems use vertically polarized, omnidirectional antennas. Platforms, such as unmanned aerial vehicles (UAVs), have additional weight and low profile constraints on the antennas. If the antenna also has a very wide bandwidth, then it can service several different frequency bands. Our goal is to build a short, vertically polarized, omni-directional, light-weight antenna that has a very wide bandwidth. We decided to use a monocone antenna as a starting point, then make changes and optimize the design to meet our goals.

Several relevant designs have appeared in the literature. The monopolar wire patch [1] and monopolar plate patch [2] are $\lambda/15$ and $\lambda/15.3$ tall respectively, but have very narrow bandwidth. The monopolar patch antenna [3] is $\lambda/11$ tall and has a very wide bandwidth. The super wideband monopolar patch [4] is similar to [3] but with an increased bandwidth. In [5] and [6] a sleeve monopole is presented. A wideband bi-cone design is presented in [7]. All these designs use shorting pins to the ground plane in order to reduce the lowest operating frequency. In a webinar session, [8], many wideband designs were presented. Of interest were planar designs like a two dimensional cone antenna, which looks like a bow tie, or other shapes such as circles or ellipses used as both ends of a dipole. These designs have a very wide bandwidth; however, the antenna height is on the order of $\lambda/5$ at the lowest frequency. In [9] and [10] a planar disk and elliptical monopole were investigated. These papers showed how the shape of the monopole, ranging from a perfect circle to an ellipse, changed the antenna input impedance and radiation characteristics. These designs slightly lowered the operating frequency compared to height, but still maintained a wide bandwidth. Reference [11] presented multiple planar monopole designs. The design with the best bandwidth had a feed shaped like a triangle. In [12], another planar monopole design showed the monopole was composed of a semi circle at the base with other stacked geometries on top. A common theme in the wideband antennas was a smooth tapered feed leading into a wide structure. These designs could be planar or volumes of revolution.

This paper presents the design of a broadband, vertically polarized, omni-directional monocone antenna that is only $\lambda/14.7$ tall. We call it the shorted top hat moncone antenna (STHMA). The next section explains the basic design of the antenna along with the numerical models and optimization process. The optimized design was built and tested. Experimental results compared well with the numerical predictions. This design was mounted on an airplane and a link budget was tested at 900 MHz and 2.4 GHz. Link budget results for the STHMA were compared with narrowband monopole antenna performance at 900 MHz and 2.4 GHz. Overall, the resulting antenna was only $\lambda/14.7$ tall at the lowest frequency and had a bandwidth of 100%.

II. Antenna Design

In order to reduce the height of the monocone antenna, a top hat was added [13]. Fig. 1 is a Microwave Studio [14] (MWS) model of a monocone antenna with a top hat over an infinite ground plane. A plot of S_{11} is shown in Fig. 3 (dashed line).

To further reduce the height and increase the bandwidth, shorting pins were inserted between the top and the infinite ground plane (Fig. 2). The design in Fig. 2 was optimized

Manuscript received December 14, 2010; revised January 15, 2012; accepted March 23, 2012. Date of publication July 05, 2012; date of current version October 02, 2012. This work was supported by ONR under Contract N00014-05-G-0106/0010.

D. W. Aten is with the Applied Research Laboratory, The Pennsylvania State University, State College, PA 16804-0030 USA (e-mail: dwa126@gmail.com).

R. L. Haupt was with the Applied Research Laboratory, The Pennsylvania State University, State College, PA 16804-0030 USA. He is now with the Colorado School of Mines, Golden, CO 80401 USA.

Color versions of one or more of the figures in this paper are available online at http://ieeexplore.ieee.org.

Digital Object Identifier 10.1109/TAP.2012.2207313

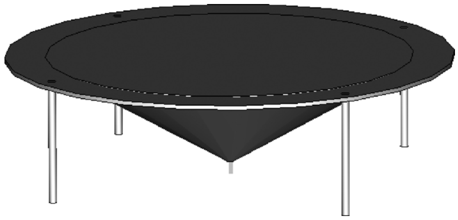

Fig. 2. An optimized design on an infinite ground plane modeled in MWS.

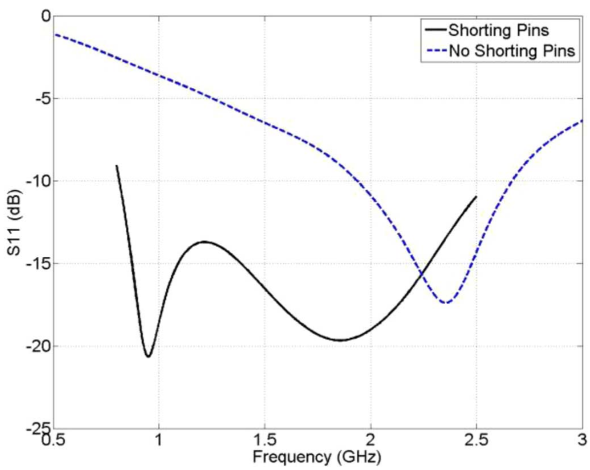

Fig. 3. S_{11} of the initial antenna design with and without shorting pins.

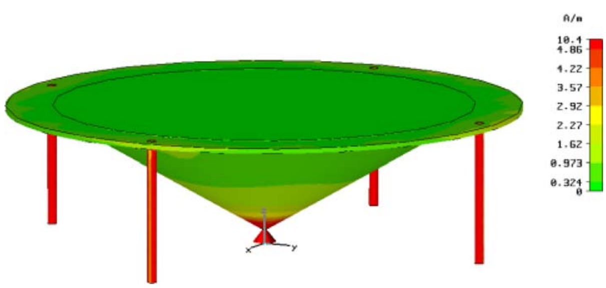

Fig. 4. Maximum surface current at 1 GHz—Infinite ground plane prototype.

using a genetic algorithm (GA) [15]. The cost function returned the peak value of S_{11} across a predefined frequency range. The overall height of the antenna is 29.3 mm. The antenna is matched ($S_{11} < -10$ dB) from 850 MHz to 2.5 GHz and is $\lambda/12$ tall at the lowest operating frequency. To understand the importance of the ground pins, both the optimized design with and without shorting pins were compared. Fig. 3 is a plot of S_{11} (solid line). By adding shorting pins to the structure, a low frequency resonance is formed at 900 MHz. This second resonance significantly increased the bandwidth of this design. Figs. 4 and 5 show the maximum surface current on the antenna at 1 GHz and 2 GHz respectively when a 1 volt source was used. The importance of the pins is seen at 1 GHz, Fig. 4, which shows there is 10.4 (A/m) of surface current present on the pins. This is almost 5 times more than at 2 GHz where the pins do not play as significant a role. This explains the resonance forming when shorting pins are used. The next step is to optimize the antenna on a finite ground plane.

Placing the antenna on a finite ground plane changes the matching and pattern characteristics of the antenna, so the antenna must be re-optimized. The size of and shape of the ground plane significantly impacts the antenna impedance and pattern. We looked at a circular and square ground plane and created a model using FEKO (Fig. 6) [16]. Fig. 7(a), (b) and (c) are the antenna pattern of the monopole modeled over an infinite ground plane, circular ground plane, and square ground plane respectively. The square and circular ground planes have a diameter and edge length of 10λ, respectively. The antenna pattern over an infinite ground plane or a circular ground plane

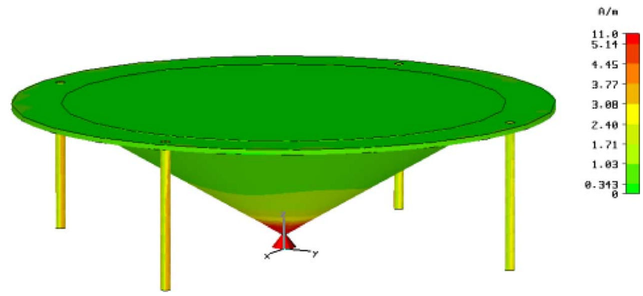

Fig. 5. Maximum surface current at 2 GHz—Infinite ground plane prototype.

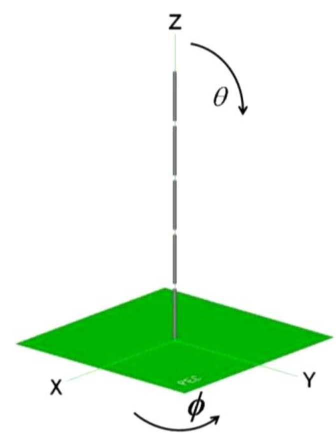

Fig. 6. A monopole antenna modeled in FEKO over an infinite ground plane.

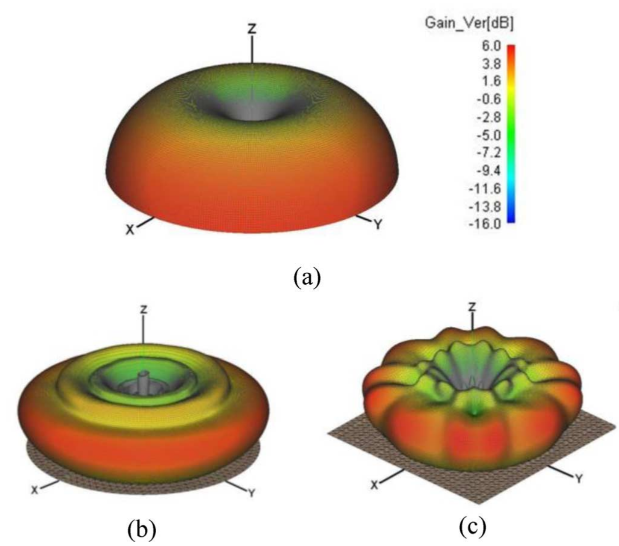

Fig. 7. The antenna pattern of a monopole modeled in FEKO over (a) infinite (b) finite circular (c) finite square ground plane.

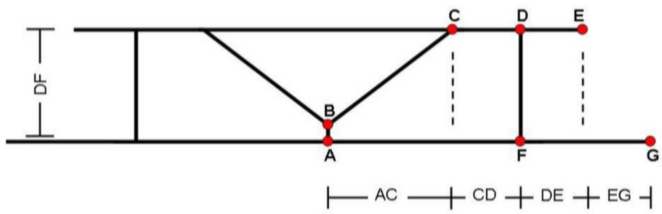

Fig. 8. The proposed antenna design showing variables used during optimization. Optimized line segment lengths: $\mathrm{DF} = 25.4, \mathrm{AC} = 45.77, \mathrm{CD} = 19.43, \mathrm{DE} = 3.14$, and $\mathrm{AG} = 126.63$ mm.

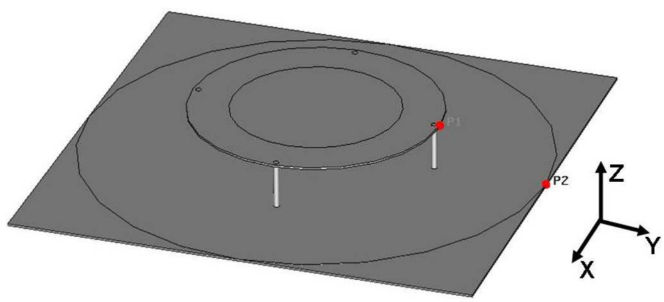

Fig. 9. A three dimensional view of the STHMA on a square ground plane modeled in MWS.

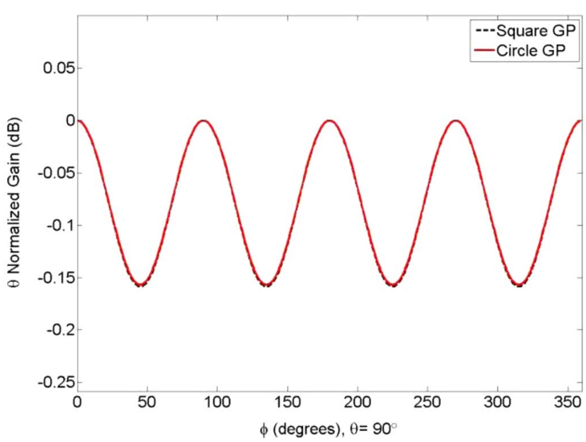

Fig. 10. 800 MHz antenna pattern comparison on a square and circular ground plane.

has no scalloping with respect to ϕ. In contrast, the antenna pattern over a square ground plane has significant scalloping with respect to ϕ. Both the antenna patterns associated with a finite ground plane have a beam squint away from the ground plane.

The antenna in Fig. 8 was optimized on a finite circular ground plane. The antenna height, DF, was set at 1 inch or 25.4 mm. Line segments AC, CD, DE, and EG were then optimized. The "best" solution had an impedance bandwidth ($S_{11} < -10$ dB) from 800 MHz to 2.4 GHz. The antenna is $\lambda/14.7$ tall at 800 MHz and $\lambda/5$ at 2.4 GHz. The antenna pattern, however, has slight scalloping due to the pins. Fig. 9 is a picture of the MWS model of the STHMA.

To reduce the scalloping in the antenna pattern, we switched to a square ground plane which had sides the same length as the diameter of the optimized solution. The corners of the ground plane pointed at $\phi = 45^\circ,\ 135^\circ,\ 225^\circ$, and 315° while the pins are at $\phi = 0^\circ,\ 90^\circ, 180^\circ$, and 270° (see Fig. 9). Figs. 10 and 11 compare the azimuth cuts of the antenna patterns when square and circular ground planes are used at 800 MHz and 2.4 GHz respectively. At 800 MHz the ground plane shape has no effect. At 2.4 GHz the square ground plane reduces the scalloping by 0.1 dB.

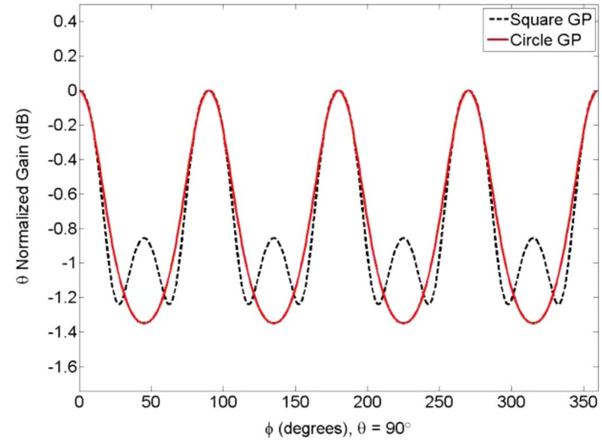

Fig. 11. 2.4 GHz antenna pattern comparison on a square and circular ground plane.

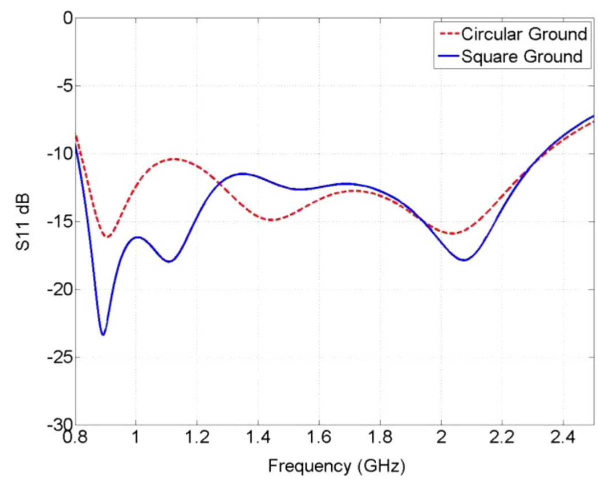

Fig. 12. Calculated S_{11} comparison using a square ground plane and a circular ground plane.

The square ground plane also improved S_{11}. Fig. 12 is a plot comparing S_{11} of a square ground plane to S_{11} of a circular ground plane. Although they both are considered matched across the same bandwidth, the square ground plane has a lower S_{11} across the entire band. As a result, we built a prototype of the STHMA over a square ground plane.

The calculated maximum gain of the STHMA is shown in Fig. 13. The gain increases starting from 1.7 dBi at 800 MHz to a max of 9 dBi at 2.4 GHz.

III. Experimental Results

An experimental model was built (Fig. 14) and tested then compared with computed results. Fig. 15 is S_{11} calculated in

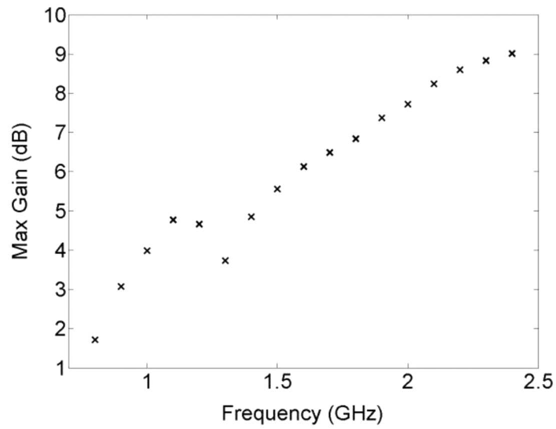

Fig. 13. Maximum gain (dBi) versus frequency of the STHMA.

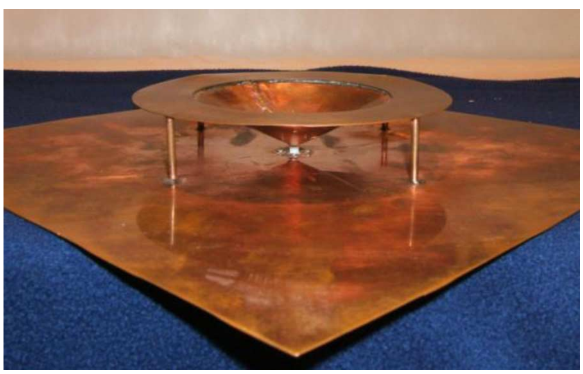

Fig. 14. A prototype of the STHMA.

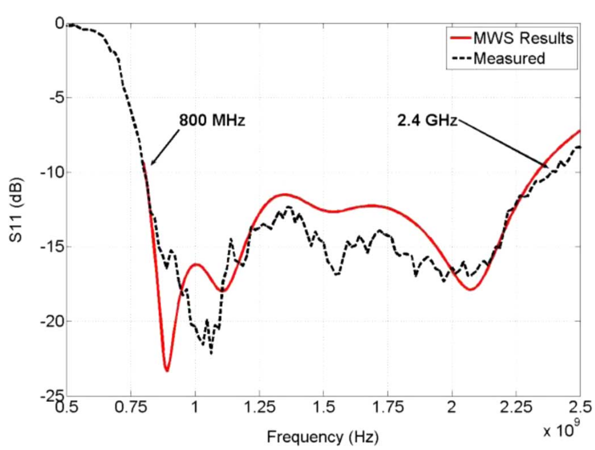

Fig. 15. Comparison of S_{11} of calculated and measured antenna.

MWS compared to measured results. The calculated and measured results are very similar. The antenna has an S_{11} less than -10 dB from 800 MHz to 2.4 GHz, which is a 3:1 bandwidth.

The antenna gains were compared to a resonant monopole at 800 MHz and 2.3 GHz over a finite ground plane the same size as the final design. Figs. 16 and 17 are comparisons of the θ gain of STHMA with a resonant monopole at 800 MHz and 2.3 GHz, respectively. The antenna patterns were taken over $\theta = 0:180$ degrees and $\phi = 0$ and 45 degrees. As frequency increases, the antenna pattern of both the monopole and STHMA squint away from the ground plane.

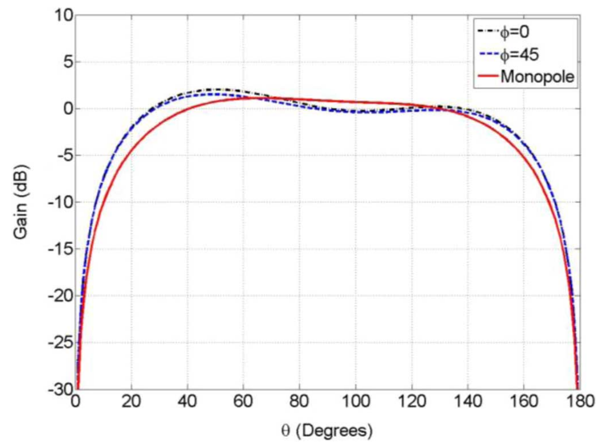

Fig. 16. STHMA θ gain (dBi) at 800 MHz compared to the gain of a resonant monopole (800 MHz) at $\phi = 0^\circ$ and 45°, $\theta = 0:180^\circ$.

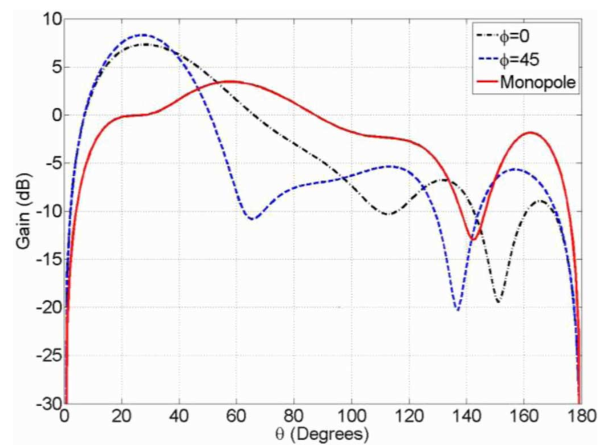

Fig. 17. STHMA θ gain (dBi) at 2.3 GHz compared to the gain of a resonant monopole (2.3 GHz) at $\phi = 0^\circ$ and 45°, $\theta = 0:180^\circ$.

The monopole antenna and STHMA pattern have similar shapes. Figs. 18 and 19 are three dimensional views of the STHMA radiation pattern at 800 MHz and 2.4 GHz, respectively. As frequency increases, the antenna pattern squints further away from the ground plane.

Antenna radiation patterns were taken in an anechoic chamber. Fig. 20 compares the calculated and measured 2D radiation patterns at 1 GHz and 2.4 GHz. Fig. 20(a) and (b) are cuts of the radiation pattern at $\theta = 90^\circ$. The antenna is omni-directional with some scalloping. Figs. 20(c) and (d) show radiation pattern cuts at $\phi = 0^\circ$ and Fig. 20(e) and (f) show radiation pattern cuts at $\phi = 45^\circ$. In all cases, the measured results compare very well to the simulated results.

IV. Link Testing

To verify that the STHMA performs, a link budget test was made to compare the antenna design to monopoles at 900 MHz and 2.4 GHz. During the test, there was a ground station that transmitted to an air station. The air station was on a Cherokee airplane, which had the STHMA antenna mounted inside a fiberglass cover on the underside of the wing (Fig. 21). The airplane had the STHMA, laptop, 900 MHz RF modem [17], 2.4 GHz RF modem [18], and GPS receiver. The ground station consisted of

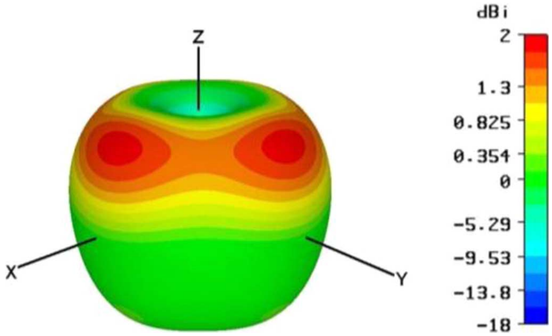

Fig. 18. 3D radiation pattern of STHMA at 800 MHz.

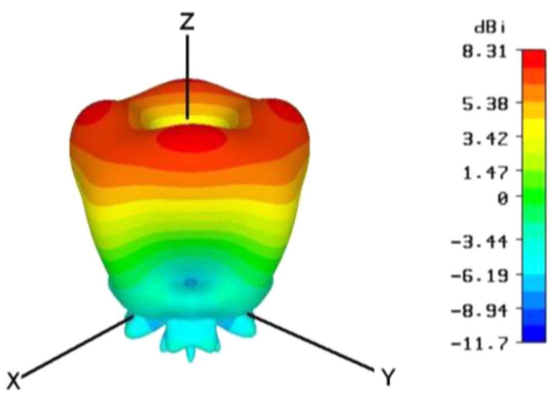

Fig. 19. 3D radiation pattern of STHMA at 2.4 GHz.

a laptop, 900 MHz RF modem, 2.4 GHz RF modem, GPS receiver, STHMA, 900 MHz 2.1 dBi gain monopole, and 2.4 GHz 2.1 dBi gain monopole. The RF modems were chosen since they covered the lower and upper bands of the antenna's range at a reasonable cost.

Four different link tests were performed with the airplane flying north to south. The first test was at 900 MHz where a resonant monopole antenna was used at the ground station. The second test was at 900 MHz where the STHMA was used at the ground station. The third test was at 2.4 GHz where a resonant monopole antenna was used at the ground station. The fourth test was at 2.4 GHz with the STHMA antenna used at the ground station.

Figs. 22 through 25 show the power level received at the air station during the 900 MHz and 2.4 GHz testing. The plot scales in the x and y directions are different: x is between 0 and 4 miles while y is between 0 and 12 miles. This scale difference magnifies the line squiggle due to the airplane motion induced by the winds. If the plots had equal axes, the paths would look very straight; however, individual paths would be hard to distinguish. The "X" indicated the position of the ground location.

Fig. 22 is the power level received in the airplane when a 900 MHz monopole antenna was used to transmit from the ground station. Fig. 23 is the power level received in the airplane when the STHMA was used to transmit at 900 MHz from the ground station. Comparing Figs. 22 and 23 it is seen that the wideband antenna has a larger coverage area than that of a 900 MHz whip.

Fig. 24 is the power level received in the airplane when a 2.4 GHz monopole antenna was used to transmit from the

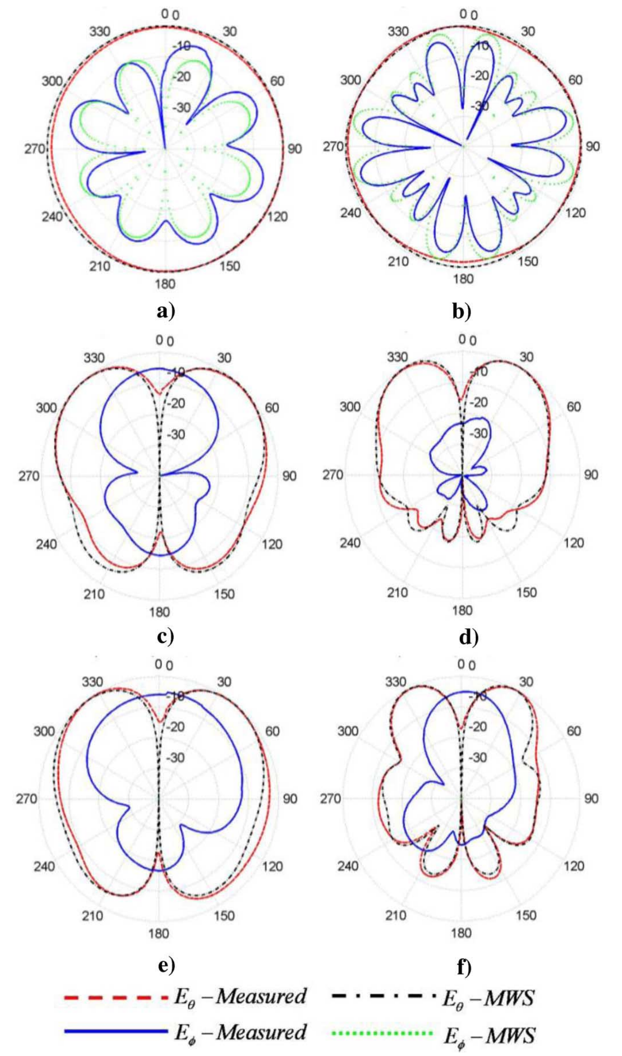

Fig. 20. STHMA normalized 2D radiation pattern measurements and comparison to MWS. (a) 1.0 GHz, ϕ 0:360, θ 90, (b) 2.4 GHz, ϕ 0:360, θ 90, (c) 1.0 GHz, ϕ 0, θ 0:360, (d) 2.4 GHz, ϕ 0, θ 0:360, (e) 1.0 GHz, ϕ 45, θ 0:360, (f) 2.4 GHz, ϕ 45, θ 0:360.

Fig. 21. STHMA mounted on the belly of a Cherokee Airplane.

ground station. Fig. 25 is the power level received in the airplane when the STHMA was used to transmit at 2.4 GHz from the ground station. Comparing Figs. 24 and 25 shows that the

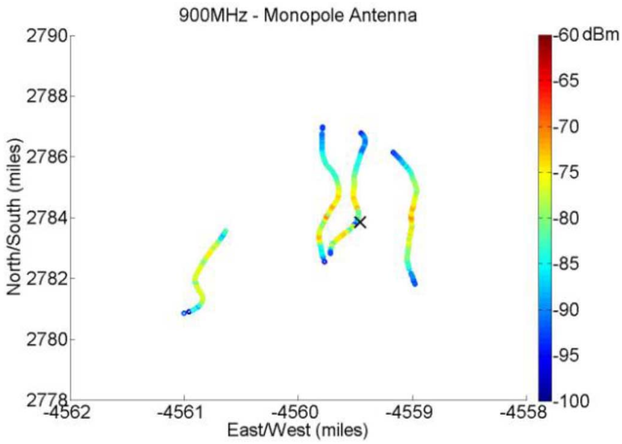

Fig. 22. Power level received when a 900 MHz, 2.1 dBi monopole is used at the ground station indicated by an "X".

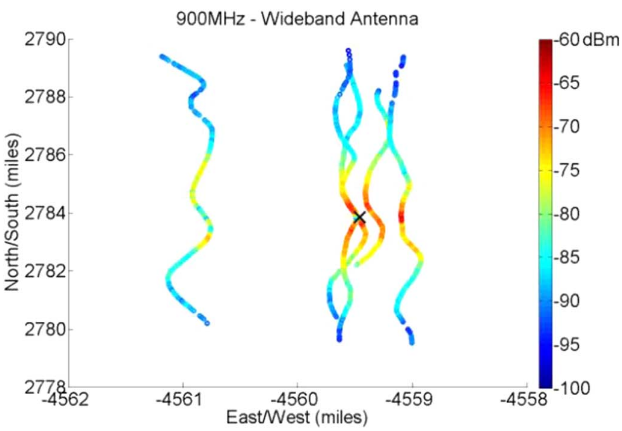

Fig. 23. Power level received at 900 MHz when the STHMA is used at the ground station indicated by an "X".

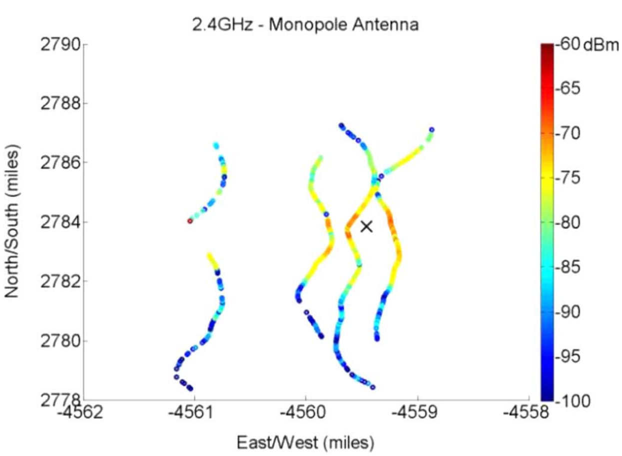

Fig. 24. Power level received when a 2.4 GHz, 2.1 dBi monopole is used at the ground station indicated by an "X".

STHMA has a similar although very slightly reduced coverage area than that of a 2.4 GHz whip.

This test demonstrates that the antenna design performed equivalent to or better than a monopole antenna at 900 MHz and 2.4 GHz. Not only did it perform well, but the antenna design was much shorter compared to wavelength.

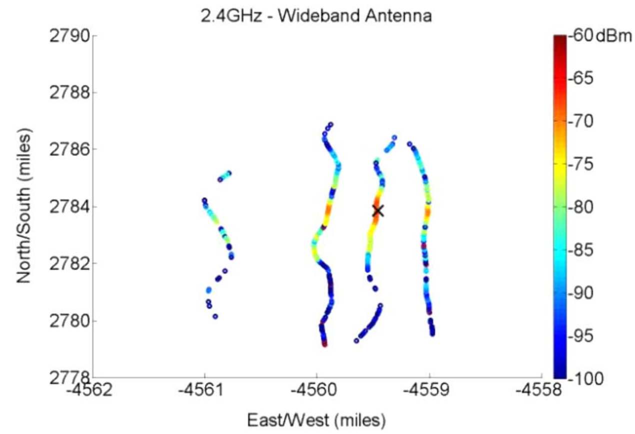

Fig. 25. Power level received at 2.4 GHz when the STHMA is used at the ground station indicated by an 'X".

TABLE I
COMPARISON OF LITERATURE AND THE STHMA PERFORMANCE

Antenna Design	Height	Bandwidth
¼ Wavelength Monopole	$\lambda/4$	9.0%
Monopolar Wire Patch[1]	$\lambda/15$	3.0%
Monopole Plate Patch[2]	$\lambda/15.3$	5.3%
Monopolar Patch Antenna[3]	$\lambda/11$	114%
Shorted Top Hat Moncone	$\lambda/14.7$	100%

V. CONCLUSION

We designed a new short, broadband, θ polarized, antenna element. The final design of the STHMA was $\lambda/14.7$ in height, θ polarized, and operated from 800 MHz to 2.4 GHz where the VSWR was less than 2:1. The antenna can be mounted on a finite ground plane such as a UAV's body and cover the same bands as 12 corresponding monopoles. Not only can it perform as well or better than the monopoles, but it is also shorter compared to wavelength across the entire band.

The STHMA height and bandwidth are compared with other similar antenna designs in Table I. It is seen that the STHMA has the height of the monopolar wire patch [1] and a bandwidth comparable to the monopolar patch antenna [3].

ACKNOWLEDGMENT

The authors would like to thank M. Foust for overseeing the fabrication process of the experimental antenna. The authors would like to thank T. Eden and J. Flemish of Penn State ARL for their support and A. Elsherbeni of University of Mississippi for performing the antenna pattern measurements.

REFERENCES

[1] Ch. Delaveeaud, Ph. Leveque, and B. Jecko, "New kind of microstrip antenna: The monopolar wire-patch antenna," *Electron. Lett.*, vol. 30, no. 1, pp. 1–2, Jan. 1994.

[2] J.-S. Row, S.-H. Yeh, and K.-L. Wong, "A wide-band monopolar plate-patch antenna," *IEEE Trans. Antennas Propag.*, vol. 50, no. 9, pp. 1328–1330, Sep. 2002.

[3] K.-L. Lau, P. Li, and K.-M. Luk, "A monopolar patch antenna with very wide impendence bandwidth," *IEEE Trans. Antennas Propag.*, vol. 53, no. 3, pp. 1004–1010, Mar. 2005.

[4] K. L. Lau, K. C. Kong, and K. M. Luk, “Super-wideband monopolar patch antenna,” *Electron. Lett.*, vol. 44, no. 12, pp. 716–718, 2008.
[5] S. L. Zuo, Y. Z. Yin, Z. Y. Zhang, and K. Song, “Enhanced bandwidth of low-profile sleeve monopole antenna for indoor base station application,” *Electron. Lett.*, vol. 46, no. 24, pp. 1587–1588, 2010.
[6] Z.-Y. Zhang, G. Fu, S.-X. Gong, S.-L. Zuo, and Q.-Y. Lu, “Sleeve monopole antenna for DVB-H applications,” *Electron. Lett.*, vol. 46, no. 13, pp. 879–880, 2010.
[7] A. K. Amert and K. W. Whites, “Miniaturization of the biconical antenna for ultrawideband applications,” *IEEE Trans. Antennas Propag.*, vol. 57, no. 12, pp. 3728–3735, 2009.
[8] S. Best, Microwave Journal and Besser Associates Webinar, “Ultrawideband antennas,” Apr. 15, 2008.
[9] M. Hammoud, P. Poey, and F. Colombel, “Matching the input impedance of a broadband disc monopole,” *Electron. Lett.*, vol. 29, no. 4, pp. 406–407, Feb. 1993.
[10] N. P. Agrawall, G. Kumar, and K. P. Ray, “Wideband planar monopole antennas,” *IEEE Trans. Antennas Propag.*, vol. 46, no. 2, pp. 294–295, Feb. 1998.
[11] M. J. Ammann and Z. N. Chen, “Wideband monopole antennas for multi-band wireless systems,” *IEEE Trans. Antennas Propag.*, vol. 45, no. 2, pp. 146–150, Apr. 2003.
[12] S.-Y. Suh, W. L. Stutzman, and W. A. Davis, “Multi-broadband monopole disc antennas,” in *Proc. IEEE Antennas Propag. Society Int. Symp. Digest*, Columbus, OH, vol. 3, pp. 616–619.
[13] A. Gangi, S. Sensiper, and G. Dunn, “The characteristics of electrically short, umbrella top-loaded antennas,” *IEEE Trans. Antennas Propag.*, vol. 13, no. 6, pp. 864–871, Nov. 1965.
[14] Sonnet Software, Inc, CST Microwave Studio Jun. 16, 2009 [Online]. Available: www.sonnetsoftware.com, version 2009.07
[15] R. L. Haupt and S. E. Haupt*, Practical Genetic Algorithms*, 2nd ed. New York: Wiley, 2004.
[16] FEKO Suite 5.4, EM Software and Systems [Online]. Available: www.feko.info 2008
[17] XTend RF Modems [Online]. Available: http://www.digi.com/products/wireless/xtend.jsp
[18] XStream RF Modems [Online]. Available: http://www.digi.com/products/wireless/xstream.jsp

Daniel W. Aten was born in Philadelphia in 1983. He received the B.S. and M.S. degrees in electrical engineering from The Pennsylvania State University (Penn State), State College, in 2006 and 2009, respectively.

He is currently a Research and Development Engineer at the Applied Research Laboratory, Pennsylvania State University, State College. Previously, he was an Antenna Design Engineer at API Technologies, State College, PA, and a Research and Development Engineer at the Applied Research Laboratory, Penn State. His research interests include wideband antenna design and electrically small antenna design.

Randy L. Haupt (M’82–SM’90–F’00) received the B.S. degree in electrical engineering from the U.S. Air Force Academy, U.S. Academy, CO, the M.S. degree in engineering management from Western New England College, Springfield, MA, in 1981, the M.S. degree in electrical engineering from Northeastern University, Boston, MA, in 1983, and the Ph.D. degree in electrical engineering from the University of Michigan, Ann Arbor, in 1987.

Currently, he is a Professor and Department Head of EECS, Colorado School of Mines, Golden. Previously, he was an RF Staff Consultant at Ball Aerospace & Technologies Corp., Westminster, CO, Senior Scientist and Department Head at the Applied Research Laboratory of Pennsylvania State University, State college, Professor and Department Head of ECE at Utah State, Professor and Chair of EE at the University of Nevada Reno, and Professor of EE at the USAF Academy. He was a Project Engineer for OTH-B radar and a Research Antenna Engineer for Rome Air Development Center early in his career. He is coauthor of the books *Practical Genetic Algorithms* (2 ed.,Wiley, 2004), *Genetic Algorithms in Electromagnetics* (Wiley, 2007), and *Introduction to Adaptive Antennas*, (SciTech, 2010), as well as the author of *Antenna Arrays a Computation Approach* (Wiley, 2010).

Dr. Haupt is a Fellow of the IEEE and the Applied Computational Electromagnetics Society (ACES). He was the Federal Engineer of the Year in 1993. He serves as an Associate Editor for the “Ethically Speaking” column in the IEEE AP-S Magazine.

射 频 和 天 线 设 计 培 训 课 程 推 荐

易迪拓培训(www.edatop.com)由数名来自于研发第一线的资深工程师发起成立，致力并专注于微波、射频、天线设计研发人才的培养；我们于 2006 年整合合并微波 EDA 网(www.mweda.com)，现已发展成为国内最大的微波射频和天线设计人才培养基地，成功推出多套微波射频以及天线设计经典培训课程和 ADS、HFSS 等专业软件使用培训课程，广受客户好评；并先后与人民邮电出版社、电子工业出版社合作出版了多本专业图书，帮助数万名工程师提升了专业技术能力。客户遍布中兴通讯、研通高频、埃威航电、国人通信等多家国内知名公司，以及台湾工业技术研究院、永业科技、全一电子等多家台湾地区企业。

易迪拓培训课程列表：http://www.edatop.com/peixun/rfe/129.html

射频工程师养成培训课程套装

该套装精选了射频专业基础培训课程、射频仿真设计培训课程和射频电路测量培训课程三个类别共 30 门视频培训课程和 3 本图书教材；旨在引领学员全面学习一个射频工程师需要熟悉、理解和掌握的专业知识和研发设计能力。通过套装的学习，能够让学员完全达到和胜任一个合格的射频工程师的要求…

课程网址：http://www.edatop.com/peixun/rfe/110.html

ADS 学习培训课程套装

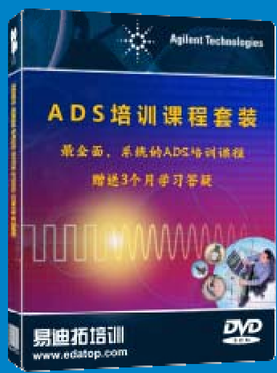

该套装是迄今国内最全面、最权威的 ADS 培训教程，共包含 10 门 ADS 学习培训课程。课程是由具有多年 ADS 使用经验的微波射频与通信系统设计领域资深专家讲解，并多结合设计实例，由浅入深、详细而又全面地讲解了 ADS 在微波射频电路设计、通信系统设计和电磁仿真设计方面的内容。能让您在最短的时间内学会使用 ADS，迅速提升个人技术能力，把 ADS 真正应用到实际研发工作中去，成为 ADS 设计专家...

课程网址： http://www.edatop.com/peixun/ads/13.html

HFSS 学习培训课程套装

该套课程套装包含了本站全部 HFSS 培训课程，是迄今国内最全面、最专业的 HFSS 培训教程套装，可以帮助您从零开始，全面深入学习 HFSS 的各项功能和在多个方面的工程应用。购买套装，更可超值赠送 3 个月免费学习答疑，随时解答您学习过程中遇到的棘手问题，让您的 HFSS 学习更加轻松顺畅…

课程网址：http://www.edatop.com/peixun/hfss/11.html

CST 学习培训课程套装

该培训套装由易迪拓培训联合微波 EDA 网共同推出，是最全面、系统、专业的 CST 微波工作室培训课程套装，所有课程都由经验丰富的专家授课，视频教学，可以帮助您从零开始，全面系统地学习 CST 微波工作的各项功能及其在微波射频、天线设计等领域的设计应用。且购买该套装，还可超值赠送 3 个月免费学习答疑…

课程网址：http://www.edatop.com/peixun/cst/24.html

HFSS 天线设计培训课程套装

套装包含 6 门视频课程和 1 本图书，课程从基础讲起，内容由浅入深，理论介绍和实际操作讲解相结合，全面系统的讲解了 HFSS 天线设计的全过程。是国内最全面、最专业的 HFSS 天线设计课程，可以帮助您快速学习掌握如何使用 HFSS 设计天线，让天线设计不再难…

课程网址：http://www.edatop.com/peixun/hfss/122.html

13.56MHz NFC/RFID 线圈天线设计培训课程套装

套装包含 4 门视频培训课程，培训将 13.56MHz 线圈天线设计原理和仿真设计实践相结合，全面系统地讲解了 13.56MHz 线圈天线的工作原理、设计方法、设计考量以及使用 HFSS 和 CST 仿真分析线圈天线的具体操作，同时还介绍了 13.56MHz 线圈天线匹配电路的设计和调试。通过该套课程的学习，可以帮助您快速学习掌握 13.56MHz 线圈天线及其匹配电路的原理、设计和调试…

详情浏览：http://www.edatop.com/peixun/antenna/116.html

我们的课程优势：

※ 成立于 2004 年，10 多年丰富的行业经验，

※ 一直致力并专注于微波射频和天线设计工程师的培养，更了解该行业对人才的要求

※ 经验丰富的一线资深工程师讲授，结合实际工程案例，直观、实用、易学

联系我们：

※ 易迪拓培训官网：http://www.edatop.com

※ 微波 EDA 网：http://www.mweda.com

※ 官方淘宝店：http://shop36920890.taobao.com